Application of electrochemical advanced oxidation to bisphenol A degradation in water. Effect of sulfate and chloride ions

Rutely Burgos-Castillo[1]*, Ignasi Sirés[2], Mika Sillanpää[1], Enric Brillas[2]*

[1] *Laboratory of Green Chemistry, School of Engineering Science, Lappeenranta University of Technology - Sammonkatu 12, FI-50130 Mikkeli, Finland*

[2] *Laboratori d'Electroquímica de Materials i del Medi Ambient, Departament de Química Física, Facultat de Química, Universitat de Barcelona, Martí i Franquès 1-11, 08028 Barcelona, Spain*

*Corresponding author: rutely.burgos.castillo@lut.fi (R. Burgos-Castillo)

brillas@ub.edu (E. Brillas)

Abstract

Electrochemical oxidation with electrogenerated H_2O_2 (EO- H_2O_2), electro-Fenton (EF), photoelectro-Fenton (PEF) and solar PEF (SPEF) have been applied to mineralize bisphenol A solutions in 0.050 M Na_2SO_4 or 0.008 M NaCl + 0.047 M Na_2SO_4 at pH 3.0. The assays were performed in an undivided cell with a boron-doped diamond (BDD) anode and an air-diffusion cathode for continuous H_2O_2 production. The PEF and SPEF processes yielded almost total mineralization due to the potent synergistic action of generated hydroxyl radicals and active chlorine, in conjunction with the photolytic action of UV radiation. The higher intensity of UV rays from sunlight explained the superior oxidation ability of SPEF. The effect of applied current density was studied in all treatments, whereas the role of bisphenol A concentration was examined in PEF. Bisphenol A abatement followed a pseudo-first-order kinetics, which was very quick in SPEF since UV light favored a large production of hydroxyl radicals from Fenton's reaction. Eight non-chlorinated and six chlorinated aromatics were identified as primary products in the chloride matrix. Ketomalonic, tartronic, maleic and oxalic acids were detected as final short-chain aliphatic carboxylic acids. The large stability of Fe(III)-oxalate complexes in EF compared to their fast photomineralization in PEF and PEF accounted for by the superior oxidation power of the latter processes.

Keywords: Bisphenol A; Electrochemical Oxidation; Electro-Fenton; Photoelectro-Fenton; Sunlight; Wastewater treatment

1. Introduction

Bisphenol A (2,2-bis(4-hydroxyphenyl)propane, $C_{15}H_{16}O_2$, M = 228.29 g mol^{-1}) is widely used in a large variety of personal care and industrial products like face lotions/cleaners, shaving creams, shampoos, body wash/lotions, sunscreen lotions, epoxy and polycarbonate resins and plastics (Umar et al., 2013; Lane et al., 2015; Bhatnagar and Anastopoulos, 2017). This chemical is considered as an endocrine disruptor and has been related to potential metabolic diseases and reproductive effects (Rochester, 2013; Chen et al., 2017; Gassman, 2017; Patel et al., 2017). These health concerns have led to the appearance of a large number of works focused on its environmental fate and stability during water treatment (Lane et al., 2015; Ebele et al., 2017; Rodriguez-Narvaez et al., 2017). Thanks to its relatively high solubility of 300 mg·L^{-1} at 25 °C in water (Careghini et al., 2015), bisphenol A has been detected at concentations up to 22 μg L^{-1} in surface water, 370 μg L^{-1} in effluents from wastewater treatment plants (WWTPs) and 1.3 μg L^{-1} in potable tap water, as well as up to 17 mg L^{-1} in landfill leachates, 95 mg kg^{-1} in sewage sludge, 10.5 mg kg^{-1} in sediments and 0.53 mg kg^{-1} in biosolids (Corrales et al., 2015; Petrie et al, 2015; Chen et al., 2017).

Several authors have reported the removal of bisphenol A from water by different methods including adsorption (Bhatnagar and Anastopoulos, 2017), ozonation (Umar et al., 2013), photo-Fenton (Molkenthin et al., 2013), electrolysis with Fe(II)-activated peroxydisulfate (Yang, 2015), UV photoelectrocatalysis (Yang et al., 2016) and solar photoelectrocatalysis (Daskalaki et al., 2013; Xiang et al., 2016). The two latter techniques are electrochemical advanced oxidation processes (EAOPs) in which organic pollutants are oxidized with the in situ generated hydroxyl radical (•OH), with ability to attack most organics up to mineralization (Martínez-Huitle et al., 2015; Moreira et al., 2017). The degradation of bisphenol A has been investigated using more potent EAOPs like electrochemical oxidation (EO) and electro-Fenton (EF). Much greater oxidation ability of

boron-doped diamond (BDD) compared to Pt, PbO_2, RuO_2 and glassy carbon anodes has been described (Murugananthan et al., 2008; Pereira et al., 2012). Total mineralization of 20 mg L^{-1} bisphenol A solutions with 0.1 M Na_2SO_4 at pH 6 was achieved by EO with BDD after 12 h of electrolysis at current density (*j*) of 35.7 mA cm^{-2}. Phenol, hydroquinone and *p*-benzoquinone were detected as intermediates (Murugananthan et al., 2008). Similarly, Pereira et al. (2012) reported total mineralization using EO with BDD when treating solutions with 150 mg L^{-1} bisphenol A and 0.1 M Na_2SO_4 at j = 30 mA cm^{-2} for 180 min, being slightly faster upon addition of 0.026 M NaCl. Li et al. (2016) found much quicker decay of 0.020 mM bisphenol A in 0.04 M NaCl as compared to 0.04 M Na_2SO_4 by EO with a Pt/stainless steel cell at *j* between 10 and 40 mA cm^{-2}. However, scarce mineralization and accumulation of chlorinated derivatives of the target molecule, phenol and *p*-benzoquinone were important drawbacks in the former medium. On the other hand, the EF treatment of O_2-saturated solutions containing 0.70 mM bisphenol A, 3.0 mM Fe^{2+} and 0.01 M HCl using a carbon felt cathode at cathodic potential of -0.55 V/SCE led to 82% mineralization, with formation of hydroxylated derivatives (Gözmen et al., 2003). More recently, Chmayssem et al. (2017) reported a 15% mineralization after 90 min of electrolysis of 100 mg L^{-1} bisphenol A in 0.05 M Na_2SO_4 at pH 3.0 using an electrochemical reactor with fixed bed of glassy carbon pellets at 0.8 A. Worth mentioning, powerful Fenton-based EAOPs with photo-assisted irradiation such as photoelectro-Fenton (PEF) and solar PEF (SPEF) have not been tested yet to treat aqueous solutions of bisphenol A. Such EAOPs could be more viable processes for the remediation of real wastewater.

This work aims to compare the mineralization of synthetic acidic bisphenol A solutions in sulfate and chloride + sulfate containing Fe^{2+} as catalyst by EAOPs like EF, PEF and SPEF using a BDD anode and an air-diffusion cathode for H_2O_2 generation. Tests without any catalyst (i.e., EO process with electrogenerated H_2O_2) (Sirés et al., 2014) were also made to

clarify the role of generated hydroxyl radicals. High-performance liquid chromatography (HPLC) was used to monitor the pollutant content decay and the evolution of final carboxylic acids. Main aromatic intermediates were identified by gas chromatography-mass spectrometry (GC-MS), allowing the proposal of a reaction route for bisphenol A degradation.

2. Experimental

2.1. Chemicals

Bisphenol A (> 99 % purity) was purchased from Sigma-Aldrich. All the other chemicals used of HPLC or analytical grade were purchased from Fluka, Panreac, Sigma-Aldrich and Acros Organics. High quality water (Millipore Milli-Q, resistivity > 18 MΩ cm) was employed for the preparation of all solutions.

2.2. Electrochemical experiments

Solutions of 150 mL of bisphenol A in 0.050 M Na_2SO_4 or 0.008 M NaCl + 0.047 M Na_2SO_4 at pH 3.0, with the same conductivity of 10 mS cm^{-1}, were treated by the different EAOPs using a cylindrical, open tank reactor under vigorous stirring. The solution was kept at 35 ºC by recirculation of external thermostated water through a jacket surrounding the tank reactor. The anode was a BDD thin-film electrode of 2.0 cm × 1.5 cm (exposed area of 3 cm^2) purchased from NeoCoat (La-Chaux-de-Fonds, Switzerland). The cathode was a 3 cm^2 circular carbon-polytetrafluoroethylene (PTFE) air-diffusion electrode purchased from Sainergy Fuel Cell (Chennai, India), mounted as reported elsewhere (Guinea et al., 2010). It provided H_2O_2 to the solution from the two-electron O_2 reduction via reaction (1) (Brillas et al., 2009; Sirés et al., 2014) upon injection of compressed air at 1 L min^{-1}. The distance between both electrodes was about 1 cm.

$$O_{2(g)} + 2H^+ + 2e^- \rightarrow H_2O_2 \quad (1)$$

The assays were conducted at constant *j* of 33.3-100 mA cm^{-2} provided by an AMEL 2051 potentiostat-galvanostat. EF, PEF and SPEF were run with 0.50 mM $FeSO_4$ since this concentration has been found optimal for analogous treatments of other organics (Ruiz et al., 2011). Solutions in PEF were exposed to irradiation by a Philips TL/6W/08 fluorescent (UVA light, λ_{max} = 360 nm) with power density of 5 W m^{-2}, measured with a Kipp&Zonen CUV 5 UV radiometer. Direct illumination in SPEF was made during the summer 2017 in our laboratory of Barcelona (latitude: 41º 23'N, longitude: 2º 10'E), with 32.6 W m^{-2} of average UV irradiance from sunlight.

2.3. Analytical procedures

The solution pH was measured on a Crison GLP 22 pH-meter. All samples were filtered prior to measurements. HPLC analysis were performed by injecting 10 μL into a Waters system composed of a 600 liquid chromatograph coupled to a 996 photodiode array detector. Bisphenol A decay was monitored by reversed-phase HPLC using a BDS Hypersil C18, 250 mm × 4.6 mm, column at 25 ºC and the photodiode detector set at λ = 254 nm. The mobile phase was 30:70 (v/v) acetonitrile:water (KH_2PO_4 10 mM, pH 3) eluted at 1.0 mL min^{-1}, appearing the peak of bisphenol A at retention time (t_r) of 3.8 min. Short-linear carboxylic acids were identified by ion-exclusion HPLC using a Bio-Rad Aminex HPX 87H, 300 mm × 7.8 mm, column at 35 ºC, and the photodiode detector selected at λ = 210 nm. A 4 mM H_2SO_4 solution was eluted at 0.6 mL min^{-1} as mobile phase. Oxalic (t_r = 6.8 min), ketomalonic (t_r = 7.4 min), tartronic (t_r=7.675) and maleic (t_r = 8.1 min) were detected. In EF, PEF and SPEF, acetonitrile (50% in volume) was added to the samples to stop the degradation process.

Total organic carbon (TOC) was determined by injecting fresh samples to a Shimadzu VCSN TOC analyzer. From TOC removal (△(TOC), in mg L^{-1}) at given time (*t*, in h) of each test at constant applied current (*I*, in A), the mineralization current efficiency (MCE, in %) was calculated from Eq. (2) (Ruiz et al., 2011):

$$\%\ \mathrm{MCE} = \frac{n\,F\,V\,\triangle(\mathrm{TOC})}{4.32\times10^{7}\,m\,I\,t}\ \times\ 100 \qquad (2)$$

where F (= 96,485 C mol^{-1}) is the Faraday constant, V represents the solution volume (in L), 4.32×10^{7} is a conversion factor (= 3,600 s h^{-1} × 12,000 mg C mol^{-1}) and m (= 15) is the number of carbon atoms of bisphenol A. An n-value of 72 was accounted for the number of electrons associated with the theoretical total mineralization as follows:

$$C_{15}H_{16}O_2 + 28H_2O \rightarrow 15CO_2 + 72H^+ + 72e^- \qquad (3)$$

Average data for replicated kinetic and mineralization assays are reported below, with small standard errors < 4% within 95% confidence interval in all cases.

Primary aromatic intermediates formed at short electrolysis time when treating 0.556 mM bisphenol A solutions in both background electrolytes at j = 100 mA cm^{-2} were identified by GC-MS using a NIST05 MS library. The organic components after each test were extracted with CH_2Cl_2 (3 × 20 mL) and the resulting solution was dried over anhydrous Na_2SO_4, filtered and concentrated up to ca. 1 mL with N_2 gas (99.99% purity). The analysis was made with the equipment and conditions previously reported by us (Steter et al., 2016), using a non-polar Teknokroma Sapiens-X5 ms column.

3. Results and discussion

3.1. Mineralization of bisphenol A solutions using 0.050 M Na_2SO_4 as the electrolyte

First, solutions of 150 mL containing 0.556 mM bisphenol A (100 mg L^{-1} TOC) in 0.050 M Na_2SO_4 at pH 3.0 were treated by EO-H_2O_2, EF and PEF at j = 33.3 mA cm^{-2} for 360 min. The two latter processes were run in the presence of 0.50 mM Fe^{2+}. In all cases, the initial colorless solution became brownish very rapidly, turning into yellow and being colorless again in less than 1 h. The colorful solutions at the beginning of these treatments suggest the

151 formation and fast destruction of complexes of Fe(III) with quinone-based intermediates
152 (Feng et al., 2013; Sirés et al., 2014). Final pH values around 2.8-2.9 informed about the
153 generation of acidic by-products such as short-linear carboxylic acids (Brillas et al., 2009; El-
154 Ghenymy et al., 2013).

155 For the above trials, Fig. 1a highlights a more rapid TOC removal in the order EO-H_2O_2
156 < EF < PEF, with reduction of 50.8%, 57.0% and 98.5% at 360 min. The slow but continuous
157 TOC removal in the former EAOP can be related to the oxidation of bisphenol A and its
158 intermediates by physisorbed BDD($^{\bullet}$OH) originated at the BDD surface from water oxidation
159 (Boye et al., 2002; Marselli et al., 2003; Özcan et al., 2008):

160 $$BDD + H_2O \rightarrow BDD(^{\bullet}OH) + H^+ + e^- \quad (4)$$

161 The larger mineralization achieved in EF can be explained by the additional production of
162 $^{\bullet}$OH from Fenton's reaction (5) between added Fe^{2+} and generated H_2O_2 (Olvera-Vargas et
163 al., 2014; Oturan and Aaron, 2014; Sirés et al., 2014), being propagated thanks to reaction (6)
164 that involves Fe^{2+} regeneration from cathodic Fe^{3+} reduction.

165 $$H_2O_2 + Fe^{2+} \rightarrow Fe^{3+} + {}^{\bullet}OH + OH^- \quad (5)$$

166 $$Fe^{3+} + e^- \rightarrow Fe^{2+} \quad (6)$$

167 It can be noted that TOC removal by EF did not differ much from that in EO-H_2O_2
168 (57.0% vs. 50.8%), which can be due to the formation of complexes of Fe(III), like Fe(III)-
169 carboxylate species that are hardly removed by BDD($^{\bullet}$OH) and $^{\bullet}$OH (Sirés et al., 2014).

170 The superiority of PEF over EF can be ascribed to the photolytic action of UVA light.
171 This radiation promotes the formation of additional amounts of $^{\bullet}$OH along with the
172 regeneration of Fe^{2+} from photolysis of $Fe(OH)^{2+}$ via reaction (7) (Flox et al., 2007; Ruiz et
173 al., 2011; Thiam et al., 2015b). A more crucial step for enhancing mineralization is the
174 photodecomposition of Fe(III) complexes with intermediates, particularly some final

carboxylic acids according to reaction (8) (El-Ghenymy et al., 2013; Pérez et al., 2017; Moreira et al., 2017).

$$Fe(OH)^{2+} + h\nu \rightarrow Fe^{2+} + {}^{\bullet}OH \quad (7)$$

$$Fe(OOCR)^{2+} + h\nu \rightarrow Fe^{2+} + CO_2 + R^{\bullet} \quad (8)$$

The fast photolysis of intermediates like Fe(III)-carboxylate complexes explains the almost total mineralization of bisphenol A with 98.5% TOC reduction achieved by PEF. This indicates that the combined action of BDD($^{\bullet}$OH) and $^{\bullet}$OH, which are the available oxidants in EF, is strongly enhanced by the photolytic action of UVA light in PEF.

Moreover, the exponential decay observed in Fig. 1a for TOC abatements suggests that they agree with a pseudo-first-order kinetics and hence, the mineralization of solutions could be controlled by the generated oxidants. The apparent rate constants (k_{TOC}) calculated from this analysis are summarized in Table 1, with their corresponding R^2. The k_{TOC}-value obtained in EO-H_2O_2 was only 1.15-fold lower than that in EF, but much lower (6.5-fold) compared to that in PEF. This trend was verified from the MCE values calculated from Eq. (2). Fig. 1b shows that the EO-H_2O_2 process achieved 14% of efficiency at times > 120 min, which could be related to a constant conversion of intermediates into CO_2. In contrast, MCE dropped largely in EF and PEF, down to 15.2% and 26.4%, respectively, with maximal of 59.7% at 120 min for the latter one. This decay in MCE at long electrolysis time can be explained by the formation of more recalcitrant molecules, along with the concomitant disappearance of organic matter (Panizza and Cerisola, 2009; Ridruejo et al., 2017).

The effect of an increase in j up to 100 mA cm^{-2} on TOC removal for the treatment of 0.556 mM bisphenol A by the same EAOPs along with SPEF process is depicted in Fig. 2a. From Table 1, at 240 min, the enhancement of TOC decay in the sequence EO-H_2O_2 < EF < PEF < SPEF was found, as also verified for the profiles obtained along the electrolyses (Fig. 2a). A close look to Table 1 confirms the same tendency from their k_{TOC}-values, which were

1.6-fold, 6.8-fold and 12.8-fold greater in EF, PEF and SPEF, respectively, as compared to EO-H_2O_2. Comparison of Fig. 1a and 2a, as well as TOC reductions at 240 min given in Table 1, allows inferring that the increase of j from 33.3 to 100 mA cm^{-2} accelerated the mineralization process in all cases. This upgrade can be ascribed to the concomitant increase in rate of all electrode reactions producing larger quantities of BDD($^{\bullet}OH$) from reaction (4) and/or $^{\bullet}OH$ from Fenton's reaction (5) as a result of the higher H_2O_2 concentration produced from reaction (1). The greater generation of such hydroxyl radicals results in a quicker formation of Fe(III) complexes that can be more rapidly photolyzed by UV light in PEF and SPEF. The higher mineralization power of SPEF compared to PEF can be explained by the much greater UV power of sunlight compared to that of the commercial UVA lamp (Salazar et al., 2012; Garcia-Segura and Brillas, 2014).

Fig. 2b confirms the degradation ability of EAOPs from the calculated MCE values, which reached 60.4% at 40 min as maximal in SPEF, further dropping to 13.2%. Table 1 also evidences a decrease in MCE of all EAOPs when j grew from 33.3 to 100 mA cm^{-2}, despite its greater oxidation ability. This behavior is common in these processes and can be explained by the increase in rate of parasitic reactions, thereby diminishing the relative contents of all hydroxyl radicals (Sirés et al., 2014; Thiam et al., 2015a, 2015b; Pérez et al., 2017).

The influence of bisphenol A concentration on the mineralization power of EAOPs was assessed for the PEF process at 100 mA cm^{-2}. Fig. 2c illustrates the rapid TOC removal found from 0.112 to 0.556 mM, yielding an almost total mineralization, with increasing TOC reductions from 93.2% to 96.6%, respectively. A higher bisphenol A content was thus beneficial. The same behavior can be established from the progressive rise in MCE, as can be seen in Fig. 2d and Table 1. The maximum MCE value of 31.7% was achieved at 60 min for 0.556 mM and, in all cases, this parameter decreased dramatically at long time, as stated above. Nevertheless, the k_{TOC}-values slightly dropped as the initial concentration was raised

225 (Table 1), because higher amounts of TOC required larger times to be abated. Since the same
226 *j* was always applied, a similar production of BDD(•OH) and •OH is expected and,
227 consequently, the lower extent to which parasitic reactions occurred allowed that a higher
228 MCE could be reached at high bisphenol A content (Ruiz et al., 2011; Thiam et al., 2015a,
229 2015b; Steter et al., 2016).

230 *3.2. Mineralization of bisphenol A solutions in chloride + sulfate medium*

231 Once clarified the degradation behavior of bisphenol A in pure sulfate medium, the study
232 was extended to a mixed electrolyte in the presence of NaCl, at pH 3.0. First assays with only
233 0.070 M NaCl (with the same conductivity as 0.050 M Na_2SO_4) showed a strong inhibition of
234 TOC removal by the EAOPs. For this reason, the effect of Cl^- was studied in 0.008 M NaCl +
235 0.047 M Na_2SO_4, a more realistic composition since urban and industrial wastewater usually
236 contains both, Cl^- and SO_4^{2-} ions. The changes of color and pH during all electrolyses were
237 similar to those found in 0.050 M Na_2SO_4.

238 Fig. 3a illustrates a rise in the oxidation ability of EAOPs in the order EO-H_2O_2 < EF <
239 PEF using the mixed matrix at 33.3 mA cm^{-2}. At 240 min, for example, 23.5%, 55.2% and
240 89.1% TOC decay was achieved for such treatments. As can be seen in Table 1, TOC
241 abatement by EO-H_2O_2 was slower in this medium, explained by the co-generation of active
242 chlorine, HClO under acidic conditions, from Cl^- oxidation at the BDD anode by reactions (9)
243 and (10) (Sirés et al., 2014; Steter at al., 2016):

244 $$2Cl^- \rightarrow Cl_{2(aq)} + 2e^- \quad (9)$$

245 $$Cl_{2(aq)} + H_2O \rightarrow HClO + Cl^- + H^+ \quad (10)$$

246 In EO-H_2O_2, bisphenol A and its products were then oxidized by both, BDD(•OH) and
247 HClO, giving rise to recalcitrant chlorinated species (as confirmed below) that usually are
248 more stable against radicals, eventually diminishing the oxidation power of this process. In

contrast, these chlorinated species were rapidly mineralized by •OH in EF, as deduced from the greater mineralization ability compared to that in sulfate medium (Table 1). In PEF, smaller TOC removals were attained in the mixed electrolyte (Table 1), suggesting the photolysis of some chloro-organics. Good linear ln TOC-time plots were obtained for these assays and the corresponding k_{TOC}-values, collected in Table 1, increased according to their relative oxidation power. The same tendency can be observed in Fig. 3b for MCE values, which decreased slightly to 10.1% and 18.9% in EO-H_2O_2 and EF, respectively, but reached 53.1% at 120 min as maximal in PEF, whereupon it dropped to 35.8% mainly due to the large loss of organic matter.

Fig. 4a illustrates the same trends at 100 mA cm^{-2}, with a clear superiority of SPEF as a result of a very positive effect of UV from sunlight, which rapidly destroys the photoactive intermediates of bisphenol A. Compared with the same treatments at 33.3 mA cm^{-2} (Fig. 3a), a notable acceleration of mineralization is evident in all cases. This enhancement with raising *j* can also be deduced from the higher k_{TOC}-values and TOC removals at 240 min (Table 1). Again, this can be ascribed to the acceleration of all electrode reactions, producing larger amounts of BDD(•OH) and/or •OH, as well as of active chlorine. Despite this, the MCE values (Fig. 4b) were always much lower than those determined at 33.3 mA cm^{-2} (Fig. 3b), as also shown in Table 1. This agrees with the concomitant increase in rate of parasitic reactions that cause the partial destruction of hydroxyl radicals. As expected, Fig. 4b shows a dramatic drop of MCE in EF, PEF and SPEF. Note that, at 100 mA cm^{-2} in EO-H_2O_2 and EF, higher k_{TOC}-values, TOC abatements and MCE values were obtained in the mixed electrolyte as compared to pure sulfate medium (Table 1). This suggests that the large generation of BDD(•OH) and/or •OH in the former matrix favors their attack over chloro-derivatives leading to fast mineralization. In contrast, the data of Table 1 show a detrimental effect of Cl^- in the case of PEF and SPEF, suggesting that the photoactivity of chlorinated products was

lower than that of non-chlorinated ones. The SPEF process yielded the fastest mineralization in both media because of the larger synergistic action of BDD(•OH), •OH, and UV.

The effect of bisphenol A concentration from 0.112 to 0.556 mM on TOC removal and MCE in the mixed electrolyte at 100 mA cm^{-2} is depicted in Fig. 4c and d, respectively. Increasing final TOC reductions from 92.0% to 96.1% with raising substrate content were found (Table 1), meaning that larger amounts of hydroxyl radicals reacted with the organic molecules rather than being destroyed by parasitic reactions. The progressively larger amounts of photoactive species thus produced can be more quickly removed upon UVA irradiation, ending in a larger mineralization. This is clear from the greater MCE values obtained at higher bisphenol A content, becoming maximal at 0.556 mM (Fig. 4d and Table 1). In contrast, the corresponding k_{TOC} values shown in Table 1 underwent a slight decrease because of the slower TOC decay as the organic load in solution was greater.

3.3. Decay of bisphenol A concentration

It has been well established that bisphenol A obeys a pseudo-first-order decay upon the action of hydroxyl radicals using EO in 0.1 M Na_2SO_4 (Murugananthan et al., 2008) and EF in 0.01 M HCl (Gözmen et al., 2003). To obtain more information about the reactivity of this compound in simultaneous events with BDD(•OH) and active chlorine, the concentration decay when treating 0.556 mM bisphenol in the mixed matrix by EO-H_2O_2 at 100 mA cm^{-2} was determined by HPLC. Fig. 5a shows a gradual and exponential abatement of this compound until it disappeared at 180 min. The inset panel of this figure evidences that a pseudo-first-order kinetics matched perfectly, with an apparent rate constant k_1 = 0.026 min^{-1} (R^2 = 0.995). This is indicative of the generation in this EAOP of a small, but steady, quantity of BDD(•OH) and active chlorine to react with bisphenol A. On the other hand, the reaction of bisphenol A with •OH in the bulk was investigated by applying the SPEF process in both media under the same experimental conditions. Fig. 5b depicts the complete bisphenol A

299 removal in only 10 min, with analogous profiles in both assays. The inset panel highlights the
300 excellent linear straights obtained for a pseudo-first-order reaction with an average k_1-value of
301 0.51±0.02 min^{-1} (R^2 ~ 0.990). The much faster removal of bisphenol A in SPEF compared to
302 EO-H_2O_2 is in agreement with the formation of a steady concentration of •OH from Fenton's
303 reaction (5), which is largely induced by photolytic reaction (7).

304 *3.4. Identification of intermediates and proposed initial reaction sequence*

305 The organic intermediates accumulated in 0.556 mM bisphenol A solutions in 0.050 M
306 Na_2SO_4 or 0.008 M NaCl + 0.047 M Na_2SO_4 treated by EO-H_2O_2 and PEF at 100 mA cm^{-2}
307 for times < 60 min were analyzed by GC-MS. In a given medium, similar compounds were
308 identified regardless of the EAOP tested. Fig. 6 presents a general initial reaction sequence
309 proposed from the 13 aromatics detected in mixed electrolyte, which could be reduced to a
310 path with 8 non-chlorinated aromatics in 0.050 M Na_2SO_4. The main oxidizing species are
311 assumed to be generated hydroxyl radicals, simplified as •OH, and active chlorine (HClO).

312 The pathway is initiated by the chlorination of bisphenol A (**1**) to yield 4,4'-
313 isopropylidene-bis(2-chlorophenol) (**2**), along with the oxidation with cleavage of its
314 isopropylidene group to form phenol (**3**), 4-isopropylphenol (**4**) and 4-*t*-butylphenol (**5**).
315 Compound **3** could be further hydroxylated in C-1 and C-4 to yield catechol (**6**) and
316 hydroquinone (**7**), respectively, or chlorinated in the same C-positions to give 2-chlorophenol
317 (**8**) and 4-chlorophenol (**9**). Subsequent chlorination of **7** leads to chlorohydroquinone (**10**),
318 whereas that of **8** or **9** yields 2,4-dichlorophenol (**11**). On the other hand, compound **4** was
319 successively oxidized/hydroxylated to 4-isopropenylphenol (**12**), 4'-hydroxyacetophenone
320 (**13**) and 2',4'-dihydroxyacetophenone (**14**). The formation of chloro-organics in the mixed
321 electrolyte is then responsible for the slower mineralization in EO-H_2O_2, PEF and SPEF.

322 The pathway of Fig. 6 cannot explain the outstanding synergistic effect of UV radiation
323 observed in PEF and SPEF, which is crucial in the mineralization processes. To clarify this,

the 0.556 mM bisphenol A solution in 0.050 M Na_2SO_4 treated by EF or PEF at 100 mA cm^{-2} was analyzed by ion-exclusion HPLC and 4 finals carboxylic acids, namely oxalic, ketomalonic, tartronic and maleic, were detected. In the Fenton-based EAOPs checked, these acids form Fe(III) complexes to a large extent (Ruiz et al., 2011; El-Ghenymy et al., 2013). It was found that the three latter acids always disappeared in less than 60 min, meaning that the Fe(III) species were rapidly destroyed by BDD(•OH) and •OH. In contrast, the Fe(III)-oxalate complexes were rapidly and completely photolyzed in PEF according to reaction (8), but they were stable in EF due to their slow destruction by BDD(•OH) and •OH, with 23.5 mg L^{-1} oxalic acid at 240 min. This represents 6.3 mg L^{-1} TOC, accounting for 20.8% of the 30.2 mg L^{-1} TOC of the final solution (Table 1). Therefore, UVA irradiation is so potent that not only photolyzes quickly Fe(III)-oxalate complexes, but also other photoactive intermediates to yield an almost total mineralization in PEF (Table 1).

4. Conclusions

PEF and SPEF treatments with a BDD/air-diffusion cell allow an almost total mineralization of bisphenol A solutions in 0.050 M Na_2SO_4 and 0.008 M NaCl + 0.047 M Na_2SO_4 at pH 3.0. This is due to the synergistic action of generated oxidizing agents (BDD(•OH), •OH and/or active chlorine) along with the photolytic action of UV radiation. The most powerful EAOP was SPEF, as result of the higher UV power provided by sunlight. The increase of *j* accelerated the mineralization, but with lower MCE, whereas the rise of bisphenol A concentration yielded greater mineralization and MCE in PEF. The bisphenol A decay always obeyed a pseudo-first-order kinetics. GC-MS analysis of treated solutions revealed the generation of 8 non-chlorinated and 6 chlorinated primary aromatics in the mixed electrolyte, demonstrating the simultaneous attack of hydroxyl radicals and chlorine active

over bisphenol A and its products. Ketomalonic, tartronic, maleic and oxalic acids were detected as final short-chain aliphatic intermediates.

Acknowledgements

The authors thank financial support from project CTQ2016-78616-R (AEI/FEDER, EU) and the fellowship awarded to R. Burgos-Castillo granted from a project supported by the Finnish Funding Agency for Innovation.

References

Bhatnagar, A., Anastopoulos, I., 2017. Adsorptive removal of bisphenol A (BPA) from aqueous solution: A review. Chemosphere 168, 885-902.

Boye, B., Michaud, P.A., Marselli, B., Dieng, M.M., Brillas, E., Comninellis, C., 2002. Anodic oxidation of 4-chlorophenoxyacetic acid on synthetic boron-doped diamond electrode. New Diamond Frontier Carbon Technol. 12, 63-72.

Brillas, E., Sirés, I., Oturan, M.A., 2009. Electro-Fenton and related electrochemical technologies based on Fenton's reaction chemistry. Chem. Rev. 109, 6570-6631.

Careghini, A., Mastorgio, A.F., Saponaro, S., Sezenna, E., 2015. Bisphenol A, nonylphenols, benzophenones, and benzotriazoles in soils, groundwater, surface water, sediments, and food: A review. Environ. Sci. Pollut. Res. 22, 5711-5741.

Chen, J., Saili, K.S., Liu, Y., Li, L., Zhao, Y., Jia, Y., Bai, C., Tanguay, R.L., Dong, Q., Huang, C., 2017. Developmental bisphenol A exposure impairs sperm function and reproduction in zebrafish. Chemosphere 169, 262-270.

Chmayssem, A., Taha, S., Hauchard, D., 2017. Scaled-up electrochemical reactor with a fixed bed three-dimensional cathode for electro-Fenton process: Application to the treatment of bisphenol A. Electrochim. Acta 225, 435-442.

370 Corrales, J., Kristofco, L.A., Steele, W.B., Yates, B.S., Breed, C.S., Williams, E.S., Brooks,
371 B.W., 2015. Global assessment of bisphenol a in the environment: Review and analysis
372 of its occurrence and bioaccumulation. Dose Response 13, 1559325815598308.
373 Daskalaki, V.M., Fulgione, I., Frontistis, Z., Rizzo, L., Mantzavinos, D., 2013. Solar light-
374 induced photoelectrocatalytic degradation of bisphenol-A on TiO_2/ITO film anode and
375 BDD cathode. Catal. Today 209, 74-78.
376 Ebele, A.J., Abou-Elwafa, M.A., Harrad, S., 2017. Pharmaceuticals and personal care
377 products (PPCPs) in the freshwater aquatic environment. Emerg. Contam. 3, 1-16.
378 El-Ghenymy, A., Oturan, N., Oturan, M.A., Garrido, J.A., Cabot, P.L., Centellas, F.,
379 Rodríguez, R.M., Brillas, E., 2013. Comparative electro-Fenton and UVA photoelectro-
380 Fenton degradation of the antibiotic sulfanilamide using a stirred BDD/air-diffusion
381 tank reactor. Chem. Eng. J. 234, 115-123.
382 Feng, L., Van Hullebusch, E.D., Rodrigo, M.A., Esposito, G., Oturan, M.A., 2013. Removal
383 of residual anti-inflammatory and analgesic pharmaceuticals from aqueous systems by
384 electrochemical advanced oxidation processes. A review. Chem. Eng. J. 228, 944-964.
385 Flox, C., Garrido, J.A., Rodríguez, R.M., Cabot, P.L., Centellas, F., Arias, C., Brillas, E.,
386 2007. Mineralization of herbicide mecoprop by photoelectro-Fenton with UVA and
387 solar light. Catal. Today 129, 29-36.
388 Garcia-Segura, S., Brillas, E., 2014. Advances in solar photoelectro-Fenton: Decolorization
389 and mineralization of the Direct Yellow 4 diazo dye using an autonomous solar pre-
390 pilot plant. Electrochim. Acta 140, 384-395.
391 Gassman, N.R., 2017. Induction of oxidative stress by bisphenol A and its pleiotropic effects.
392 Environ. Mol. Mutagen. 58, 60-71.

393 Gözmen, B., Oturan, M.A., Oturan, N., Erbatur, O., 2003. Indirect electrochemical treatment
394 of bisphenol A in water via electrochemically generated Fenton's reagent. Environ. Sci.
395 Technol. 37, 3716-3723.
396 Guinea, E., Garrido, J.A., Rodríguez, R.M., Cabot, P.L., Arias, C., Centellas, F., Brillas, E.,
397 2010. Degradation of the fluoroquinolone enrofloxacin by electrochemical advanced
398 oxidation processes based on hydrogen peroxide electrogeneration. Electrochim. Acta 55,
399 2101-2115.
400 Lane, R.F., Adams, C.D., Randtke, S.J., Carter, R.E., 2015. Bisphenol diglycidyl ethers and
401 bisphenol A and their hydrolysis in drinking water. Water Res. 72, 331-339.
402 Li, H., Long, Y., Wang, Y., Zhu, C., Ni, J., 2016. Electrochemical degradation of bisphenol A
403 in chloride electrolyte—Factor analysis and mechanisms study. Electrochim. Acta 222,
404 1144-1152.
405 Marselli, B., Garcia-Gomez, J., Michaud, P.A., Rodrigo, M.A., Comninellis, C., 2003.
406 Electrogeneration of hydroxyl radicals on boron-doped diamond electrodes. J.
407 Electrochem. Soc. 150, D79-D83.
408 Martínez-Huitle, C.A., Rodrigo, M.A., Sirés, I., Scialdone, O., 2015. Single and coupled
409 electrochemical processes and reactors for the abatement of organic water pollutants: A
410 critical review. Chem. Rev. 115, 13362–13407.
411 Molkenthin, M., Olmez-Hanci, T., Jekel, M.R., Arslan-Alaton, I., 2013. Photo-Fenton-like
412 treatment of BPA: Effect of UV light source and water matrix on toxicity and
413 transformation products. Water Res. 47, 5052-5064.
414 Moreira, F.C., Boaventura, R.A.R., Brillas, E., Vilar, V.J.P., 2017. Electrochemical advanced
415 oxidation processes: A review on their application to synthetic and real wastewaters.
416 Appl. Catal. B: Environ. 202, 217-261.

417 Murugananthan, M., Yoshihara, S., Rakuma, T., Shirakashi, T., 2008. Mineralization of
418 bisphenol A (BPA) by anodic oxidation with boron-doped diamond (BDD) electrode. J.
419 Hazard. Mater. 154, 213-220.
420 Olvera-Vargas, H., Oturan, N., Brillas, E., Buisson, D., Esposito, G., Oturan, M.A., 2014.
421 Electrochemical advanced oxidation for cold incineration of the pharmaceutical
422 ranitidine: Mineralization pathway and toxicity evolution. Chemosphere 117, 644-651.
423 Oturan, M.A., Aaron, J.J., 2014. Advanced oxidation processes in water/wastewater
424 treatment: Principles and applications. A review. Crit. Rev. Environ. Sci. Technol. 44,
425 2577-2641.
426 Özcan, A., Şahin, Y., Koparal, A.S., Oturan, M.A., 2008. Propham mineralization in aqueous
427 medium by anodic oxidation using boron-doped diamond anode. Experimental
428 parameters' influence on degradation kinetics and mineralization efficiency. Water Res.
429 42, 2889-2898.
430 Panizza, M., Cerisola, G., 2009. Direct and mediated anodic oxidation of organic pollutants.
431 Chem. Rev. 109, 6541-6569.
432 Patel, S., Brehm, E., Gao, L., Rattan, S., Ziv-Gal, A., Flaws, J.A., 2017. Bisphenol A
433 exposure, ovarian follicle numbers, and female sex steroid hormone levels: results from
434 a CLARITY-BPA study. Endocrinology 158, 1727-1738.
435 Pereira, G.F., Rocha-Filho, R.C., Bocchi, N., Biaggio, S.R., 2012. Electrochemical
436 degradation of bisphenol A using a flow reactor with a boron-doped diamond anode.
437 Chem. Eng. J. 198-199, 282-288.
438 Pérez, T., Sirés, I., Brillas, E., Nava, J.L., 2017. Solar photoelectro-Fenton flow plant
439 modeling for the degradation of the antibiotic erythromycin in sulfate medium.
440 Electrochim. Acta 228, 45-56.

441 Petrie, B., Barden, R., Kasprzyk-Hordern, B., 2015. A review on emerging contaminants in
442 wastewaters and the environment: Current knowledge, understudied areas and
443 recommendations for future monitoring. Water Res. 72, 3-27.
444 Ridruejo, C., Salazar, C., Cabot, P.L., Centellas, F., Brillas, E., Sirés, I., 2017.
445 Electrochemical oxidation of anesthetic tetracaine in aqueous medium. Influence of the
446 anode and matrix composition. Chem. Eng. J. 326, 811-819.
447 Rochester, J.R., 2013. Bisphenol A and human health: A review of the literature. Reprod.
448 Toxicol. 42, 132-155.
449 Rodriguez-Narvaez, O.M., Peralta-Hernandez, J.M., Goonetilleke, A., Bandala, E.R., 2017.
450 Treatment technologies for emerging contaminants in water: A review. Chem. Eng. J.
451 323, 361-380.
452 Ruiz, E.J., Hernández-Ramírez, A., Peralta-Hernández, J.M., Arias, C., Brillas, E., 2011.
453 Application of solar photoelectro-Fenton technology to azo dyes mineralization: Effect of
454 current density, Fe^{2+} and dye concentration. Chem. Eng. J. 171, 385-392.
455 Salazar, R., Brillas, E., Sirés, I., 2012. Finding the best Fe^{2+}/Cu^{2+} combination for the solar
456 photoelectro-Fenton treatment of simulated wastewater containing the industrial textile
457 dye Disperse Blue 3. Appl. Catal. B: Environ. 115-116, 107-116.
458 Sirés, I., Brillas, E., Oturan, M.A., Rodrigo, M.A., Panizza, M., 2014. Electrochemical
459 advanced oxidation processes: today and tomorrow. A review. Environ. Sci. Pollut. Res.
460 21, 8336-8367.
461 Steter, J.R., Brillas, E., Sirés, I., 2016. On the selection of the anode material for the
462 electrochemical removal of methylparaben from different aqueous media. Electrochim.
463 Acta 222, 1464-1474.

Thiam, A. Brillas, E., Centellas, F., Cabot, P.L., Sirés, I., 2015a. Electrochemical reactivity of Ponceau 4R (food additive E124) in different electrolytes and batch cells. Electrochim. Acta 173, 523-533.

Thiam, A., Sirés, I., Brillas, E., 2015b. Treatment of a mixture of food color additives (E122, E124 and E129) in different water matrices by UVA and solar photoelectro-Fenton. Water Res. 81, 178-187.

Umar, M., Roddick, F., Fan, L., Aziz, H.A., 2013. Application of ozone for the removal of bisphenol A from water and wastewater - A review. Chemosphere 90, 2197-2207.

Xiang, G., Yu, Z., Hou, Y., Chen, Y., Peng, Z., Sun, L., Sun, L., 2016. Simulated solar-light induced photoelectrocatalytic degradation of bisphenol-A using Fe^{3+}-doped TiO_2 nanotube arrays as a photoanode with simultaneous aeration. Sep. Purif. Technol. 161, 144-151.

Yang, C., 2015. Degradation of bisphenol A using electrochemical assistant Fe(II)-activated peroxydisulfate process. Water Sci. Eng. 8, 139-144.

Yang, L., Li, Z., Jiang, H., Jiang, W., Su, R., Luo, S., Luo, Y., 2016. Photoelectrocatalytic oxidation of bisphenol A over mesh of TiO_2/graphene/Cu_2O. Appl. Catal. B: Environ. 183, 75-85.

Figure captions

Fig. 1. Change of (a) TOC and (b) mineralization current efficiency with electrolysis time during the treatment of 150 mL of 0.556 mM bisphenol A in 0.050 M Na_2SO_4 at pH 3.0 using a boron-doped diamond (BDD)/air-diffusion cell (3 cm^2 electrode area) at j = 33.3 mA cm^{-2} and 35 ºC. Method: (●) Electrochemical oxidation with electrogenerated H_2O_2 (EO-H_2O_2), (■) electro-Fenton (EF) with 0.50 mM Fe^{2+} and (▲) photoelectro-Fenton (PEF) with 0.50 mM Fe^{2+} using a 6 W UVA lamp.

Fig. 2. Time course of (a,c) TOC and (b,d) mineralization current efficiency during the degradation of 150 mL of bisphenol A solutions in 0.050 M Na_2SO_4 at pH 3.0 and 35 ºC using a BDD/air-diffusion cell at j = 100 mA cm^{-2}. (a,b) 0.556 mM bisphenol A treated by: (●) EO-H_2O_2 and (■) EF, (▲) PEF and (▼) solar photoelectro-Fenton (SPEF) with 0.50 mM Fe^{2+}. (c,d) PEF process with: (●) 0.112 mM, (■) 0.278 mM, (▼) 0.417 mM and (▲) 0.556 mM bisphenol A.

Fig. 3. Variation of (a) TOC and (b) mineralization current efficiency with electrolysis time for the treatment of 150 mL of 0.556 mM bisphenol A in 0.008 M NaCl + 0.047 M Na_2SO_4 at pH 3.0 using a BDD/air-diffusion cell at j = 33.3 mA cm^{-2} and 35 ºC. Method: (●) EO-H_2O_2, (■) EF and (▲) PEF.

Fig. 4. (a,c) TOC and (b,d) mineralization current efficiency vs. electrolysis time under the same conditions of Fig. 2 but using 0.008 M NaCl + 0.047 M Na_2SO_4 as electrolyte. (a,b) 0.556 mM bisphenol A treated by: (●) EO-H_2O_2, (■) EF, (▲) PEF and (▼) SPEF. (c,d) PEF process with: (●) 0.112 mM, (■) 0.278 mM, (▼) 0.417 mM and (▲) 0.556 mM bisphenol A.

Fig. 5. Time course of bisphenol A concentration during the degradation of 150 mL of 0.556 mM bisphenol A in different electrolytes at pH 3.0 using a BDD/air-diffusion cell at j = 100 mA cm^{-2} and 35 ºC. (a) EO-H_2O_2 with 0.008 M NaCl + 0.047 M Na_2SO_4. (b) SPEF with (▽) 0.050 M Na_2SO_4 and (○) 0.008 M NaCl + 0.047 M Na_2SO_4. The inset panels present the corresponding pseudo-first-order kinetic analysis.

Fig. 6. Initial reaction sequence proposed for bisphenol A degradation in the Cl-containing matrix by EAOPs. $^{\bullet}OH$ accounts for hydroxyl radicals originated at the anode surface and from Fenton's reaction, whereas HClO accounts for active chlorine formed from Cl^{-} oxidation at the anode.

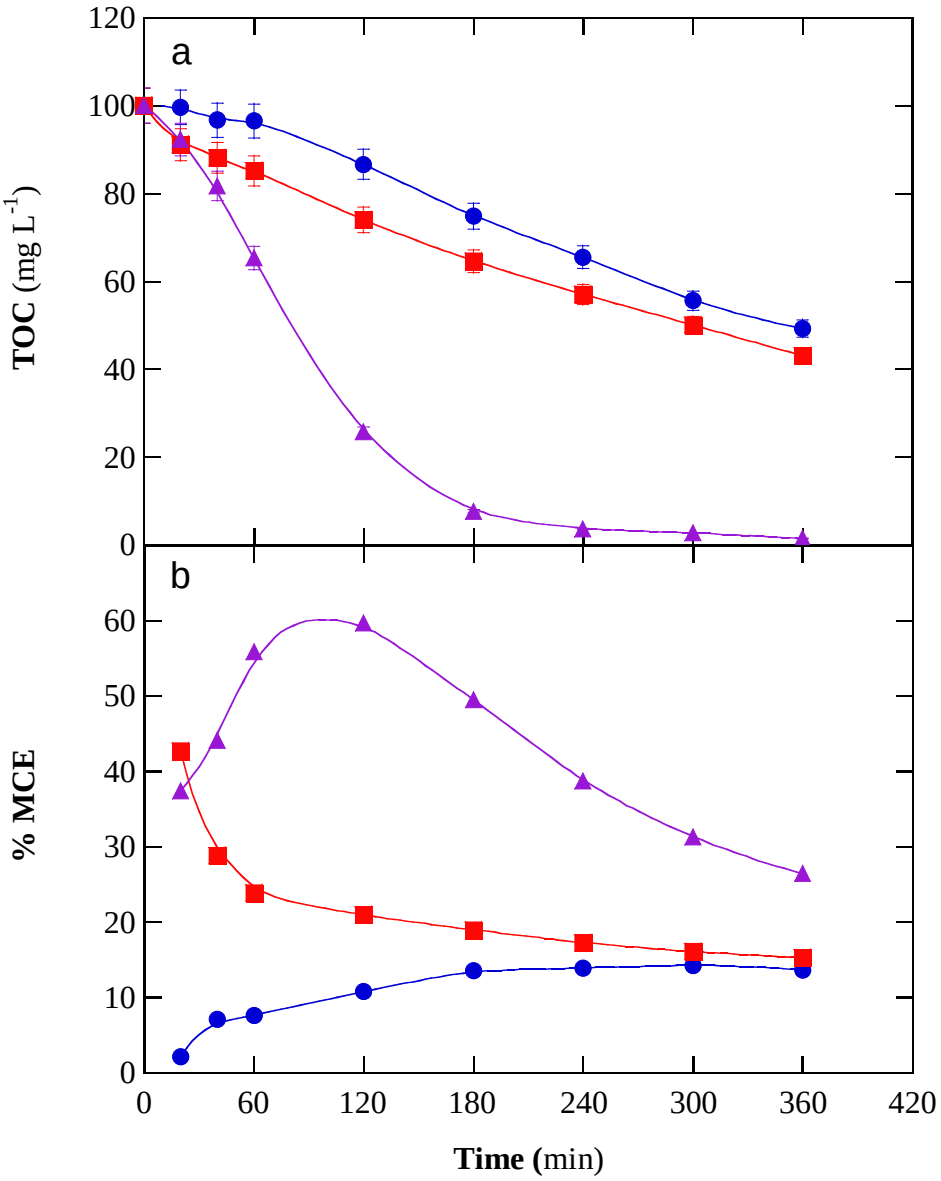
a
b
TOC (mg L-1)
% MCE
Time (min)
0
20
40
60
80
100
120
0
10
20
30
40
50
60
0
60
120
180
240
300
360
420

Fig. 1

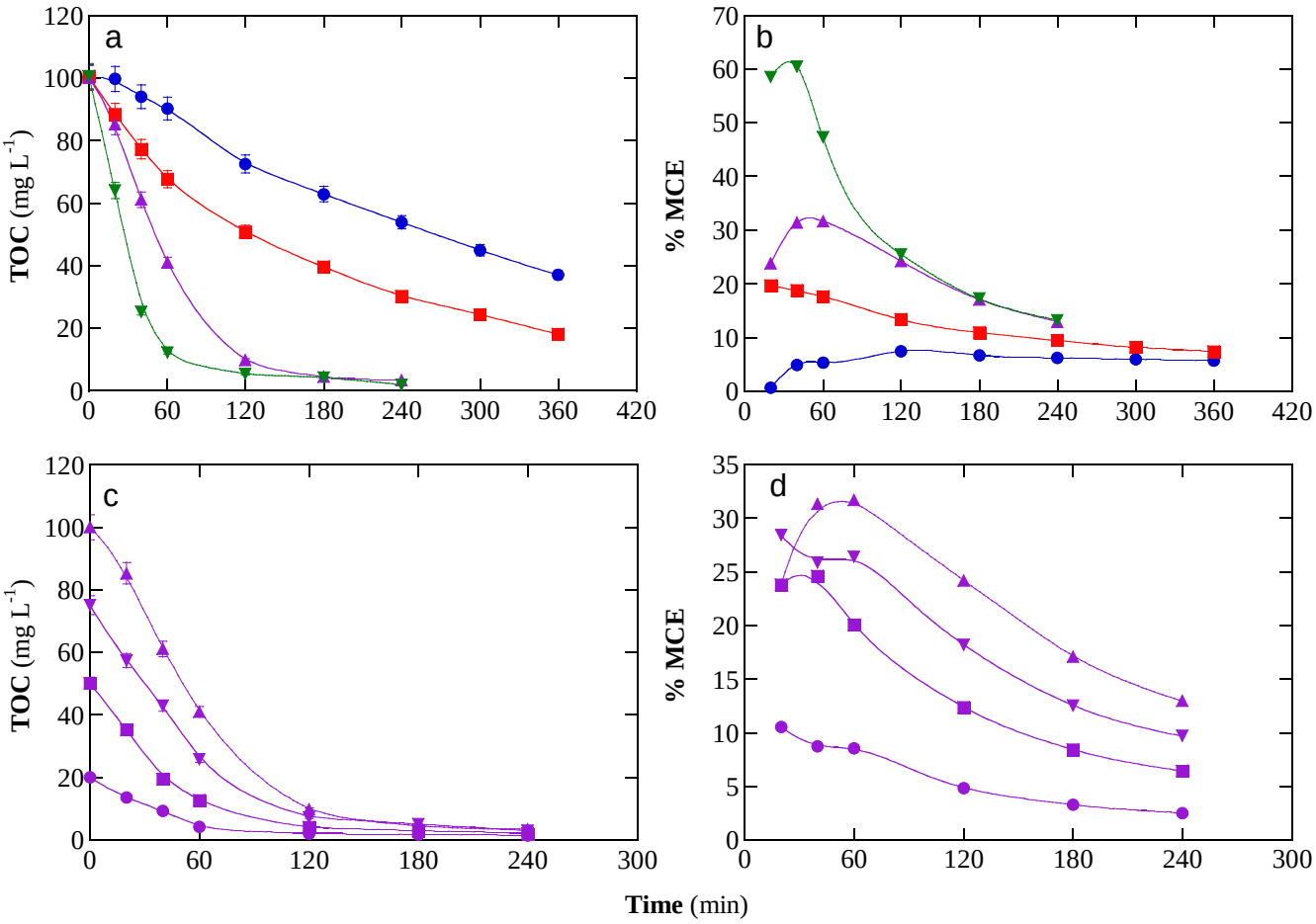

Fig. 2

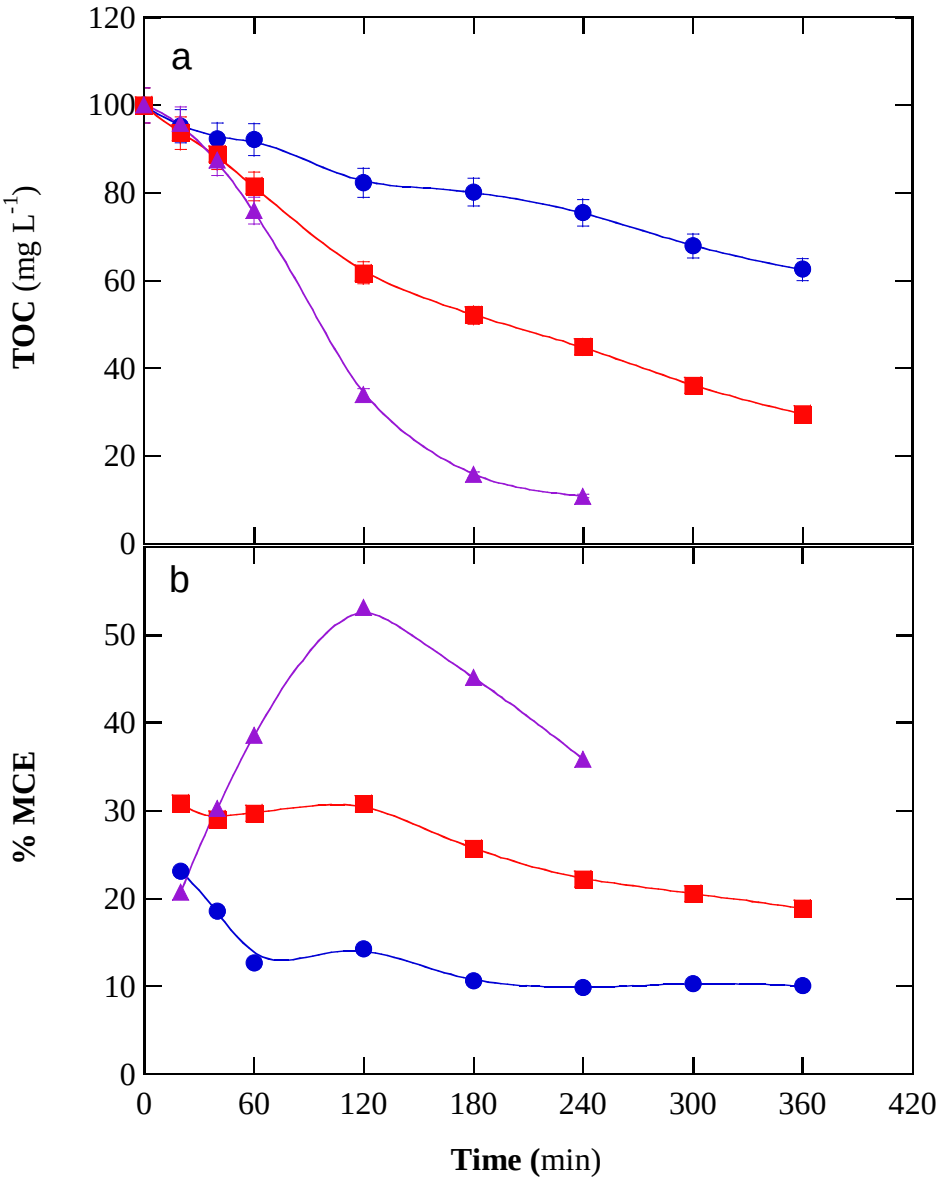
a
b
TOC (mg L-1)
% MCE
Time (min)
0
20
40
60
80
100
120
10
30
50
0
60
120
180
240
300
360
420

Fig. 3

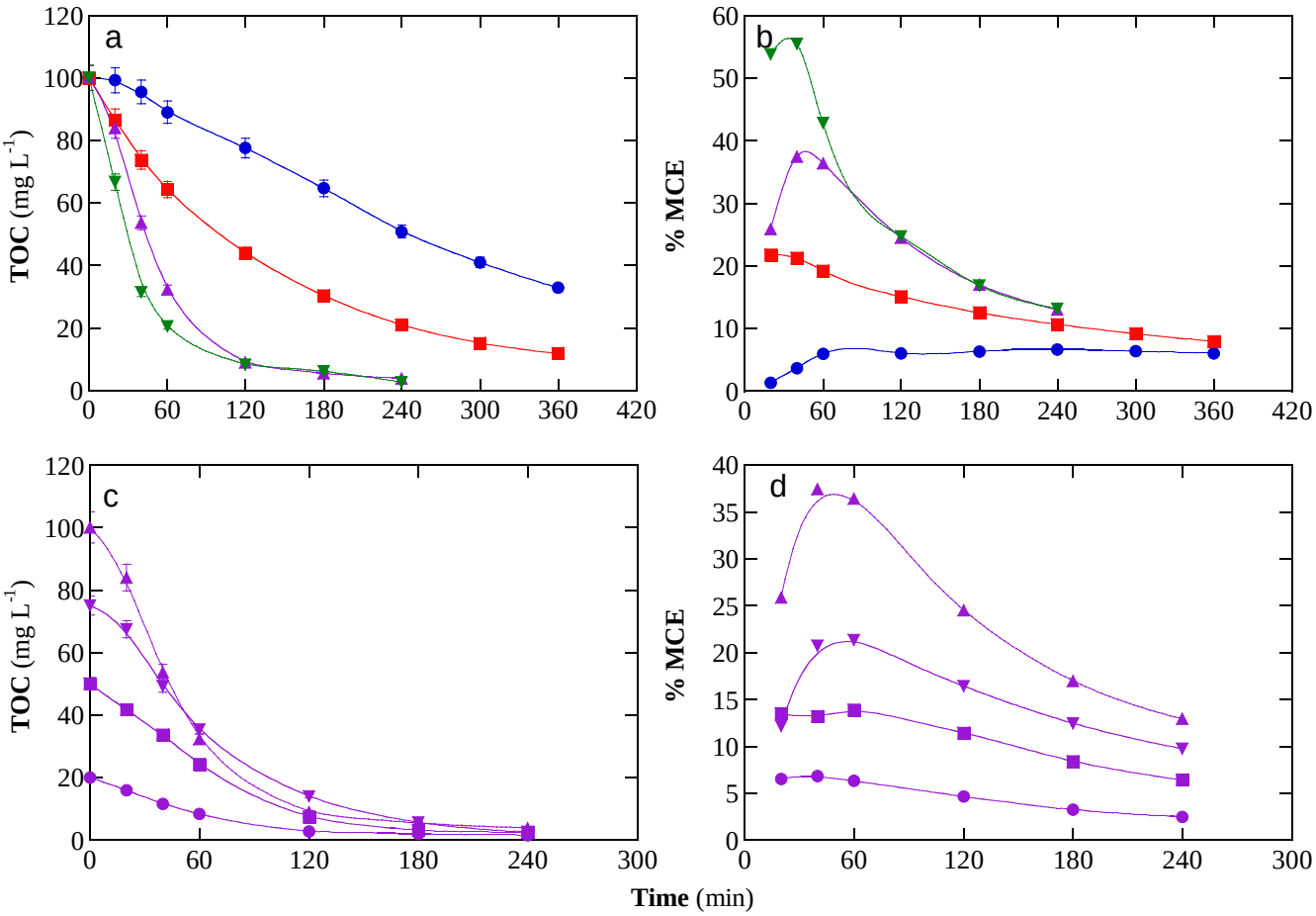

Fig. 4

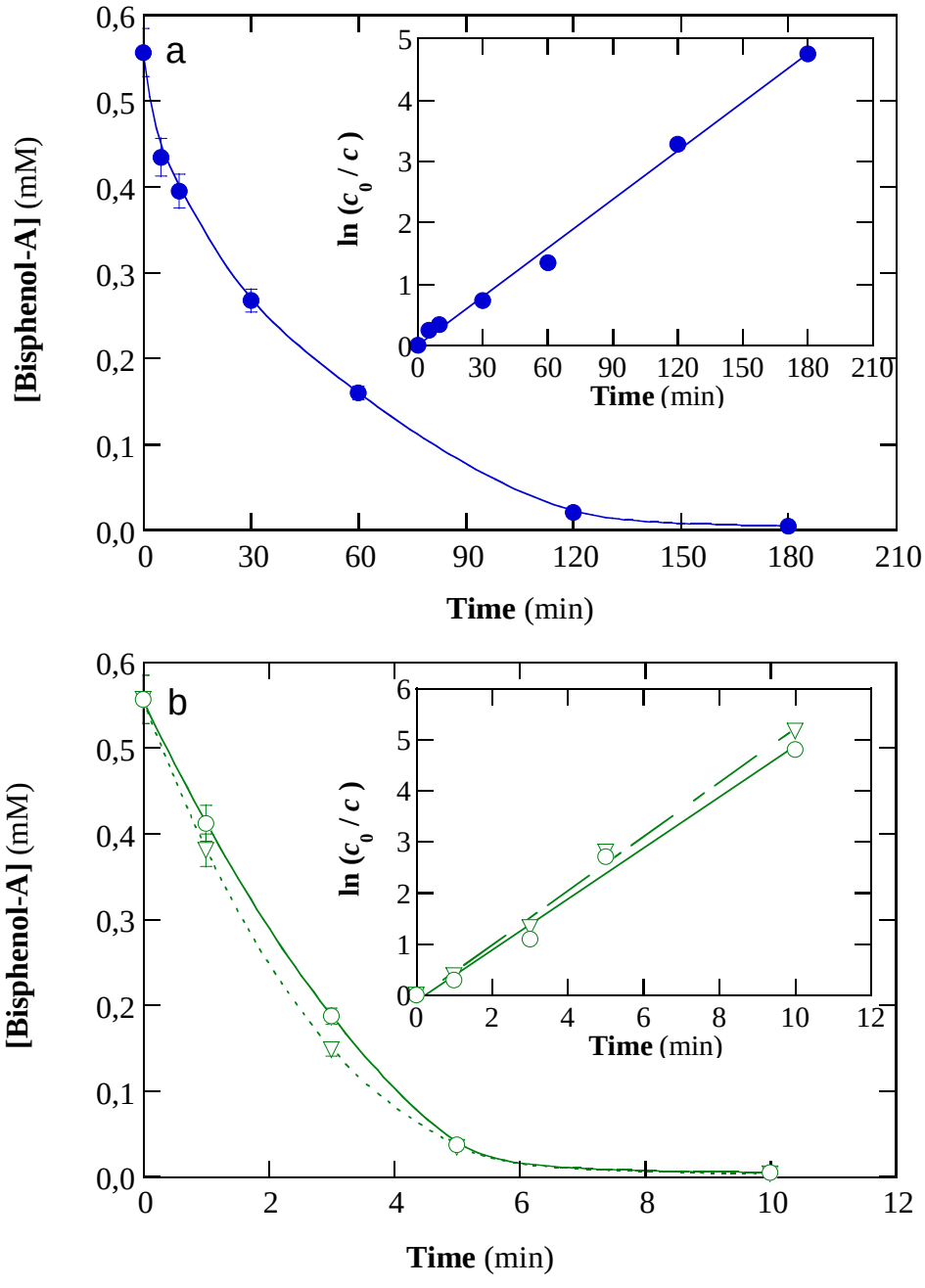
a
[Bisphenol-A] (mM)
Time (min)
ln (c0 / c)
Time (min)
b
[Bisphenol-A] (mM)
Time (min)
ln (c0 / c)
Time (min)

Fig. 5

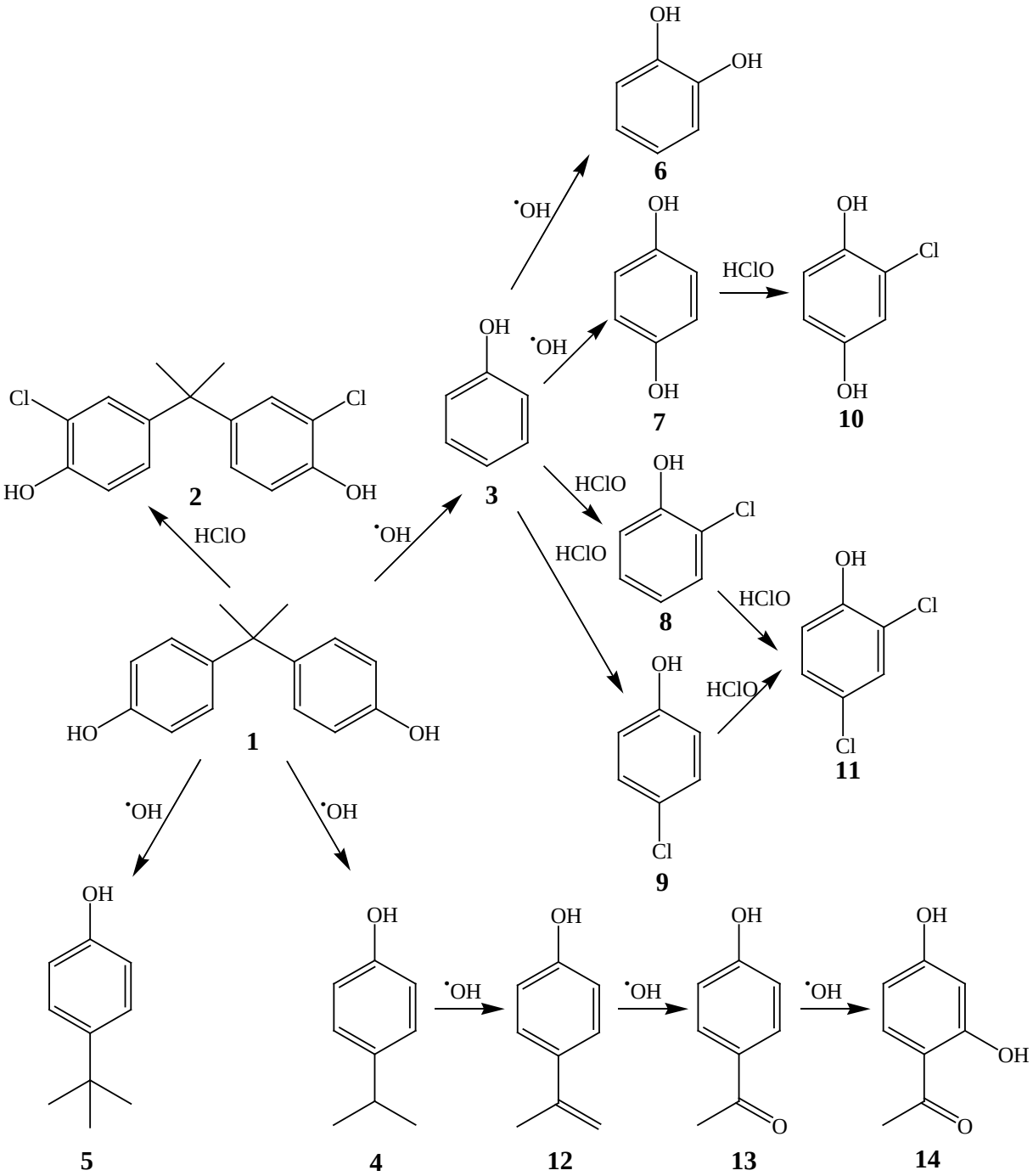
OH
OH
6
•OH
OH
OH
Cl
HClO
OH
•OH
OH
OH
7
10
Cl
Cl
HO
OH
2
3
HClO
OH
Cl
HClO
8
HClO
OH
Cl
HClO
OH
HO
OH
1
HClO
11
Cl
9
•OH
•OH
OH
OH
OH
OH
•OH
•OH
•OH
OH
O
O
5
4
12
13
14

Fig. 6

Table 1.

Pseudo-first-order rate constant obtained for TOC removal (k_{TOC}) and the corresponding *R*-squared, and percentage of TOC removal and mineralization current efficiency at 240 min. Trials were made using 150 mL of bisphenol A solutions in different matrices at pH 3.0 and 35 ºC with different electrolytes by several EAOPs with a BDD/air-diffusion cell.

Method	$[\text{Bisphenol A}]_0$ (mM)	j (mA cm^{-2})	k_{TOC} (min^{-1})	R^2	% TOC removal	% MCE
0.050 M Na_2SO_4						
EO-H_2O_2	0.556	33.3	2.0×10^{-3}	0.985	34.6	13.9
	0.556	100	2.8×10^{-3}	0.996	46.2	6.2
EF[a]	0.556	33.3	2.3×10^{-3}	0.998	43.0	17.3
	0.556	100	4.6×10^{-3}	0.995	69.8	9.4
PEF[a,b]	0.556	33.3	1.3×10^{-2}	0.980	96.3	38.7
	0.112	100	2.3×10^{-2}	0.979	93.2	2.5
	0.278	100	2.1×10^{-2}	0.994	95.9	6.4
	0.417	100	2.0×10^{-2}	0.995	96.3	9.7
	0.556	100	1.9×10^{-2}	0.987	96.6	12.9
SPEF[a,c]	0.556	100	3.6×10^{-2}	0.985	98.2	13.2
0.008 M NaCl + 0.047M Na_2SO_4						
EO-H_2O_2	0.556	33.3	1.2×10^{-3}	0.986	23.5	9.8
	0.556	100	3.1×10^{-3}	0.990	49.2	6.6
EF[a]	0.556	33.3	3.4×10^{-3}	0.996	55.2	22.2
	0.556	100	6.0×10^{-3}	0.985	79.1	10.6
PEF[a,b]	0.556	33.3	1.0×10^{-2}	0.981	89.1	35.8
	0.112	100	1.7×10^{-2}	0.994	92.0	2.4
	0.278	100	1.6×10^{-2}	0.983	95.2	6.5
	0.417	100	1.5×10^{-2}	0.997	96.0	9.6
	0.556	100	1.4×10^{-2}	0.990	96.1	12.8
SPEF[a,c]	0.556	100	2.8×10^{-2}	0.985	97.4	13.1

[a] Addition of 0.50 mM Fe^{2+}

[b] Upon 6 W UVA irradiation

[c] Upon sunlight irradiation